

Experimental Testing and Numerical Modelling Validation for Ranque-Hilsch Vortex Cooling Tube Design

¹Joseph Akpan, ²Edwin Effiong, ¹Oludolapo Akanni, ²Victor Okorie

¹Department of Industrial Engineering
Durban University of Technology
Durban, SA
¹22176142@dut4life.ac.za, ¹OludolapoO@dut.ac.za

²Department of Mechanical Engineering
University of Uyo
Uyo, Nigeria
²edwinumoeffiong@gmail.com, ²victorokorie24@gmail.com

Abstract

Space cooling has a long history of adopting unconventional ways. The vortex tube cooling system (VTCS), a non-traditional cooling system with no moving parts, is the subject of this research. It was designed using CAD and parameters culled from the literature. This system's design includes a control valve, and a cold air orifice. To achieve the best cooling effect, unplasticized polyvinyl chloride (uPVC) material was employed in the design. By employing the hot and cold ends of the tube, it was feasible to segregate warm and cold air. The amount of hot air discharged through the tube was varied to experiment a hot-air/cold-air mass fraction for the most cooling at different inlet pressures. In these two sets of testing, the inlet air pressure and mass percentage of hot air in the vortex tube were investigated. In the design of the vortex tube, ABAQUS finite element software was used (for simulation/visualization of properties such as pressure distribution, temperature distribution, and velocity) for both comparative and validation reasons. Physical experimentation yielded a temperature of 22.3°C, which was 9.4°C lower than the entrance air temperature. The finite element simulation projected a lower temperature of 19°C. When the hot air mass percentage was set to 80%, both the simulated model and the prototype showed the best cooling performance. At maximum cooling with an 80 percent hot air mass fraction, the input air pressure for the prototype and simulated model was 4 bar and 2.6 bar, respectively.

Keywords

Ranque-Hilsch Vortex Tube, Simulation, Cooling, Design

1. Introduction

The development of an alternate cooling approach has become imminent to compete with or completely replace vapor compression, which is not as environmentally friendly as space cooling and near-room temperature refrigeration applications, at least in part. The air conditioning and refrigeration (hereafter, "industry") industry is facing increased expectations for energy efficiency and reduced environmental impact.(Brown & Domanski, 2011) Low-promise cooling options, absorption cooling, desiccant cooling, mechanical cooling, magnetic cooling, thermoacoustic cooling, thermoelectric cooling, trans-critical CO₂, are typical types of alternative cooling technologies that have been developed over the years to contribute to reducing the greenhouse effect gases because of conventional generation of cooling from refrigerants such as Chlorofluorocarbons (CFCs), and hydrochlorofluorocarbons (HCFCs). Some of the cooling technologies are shown in figure 1.

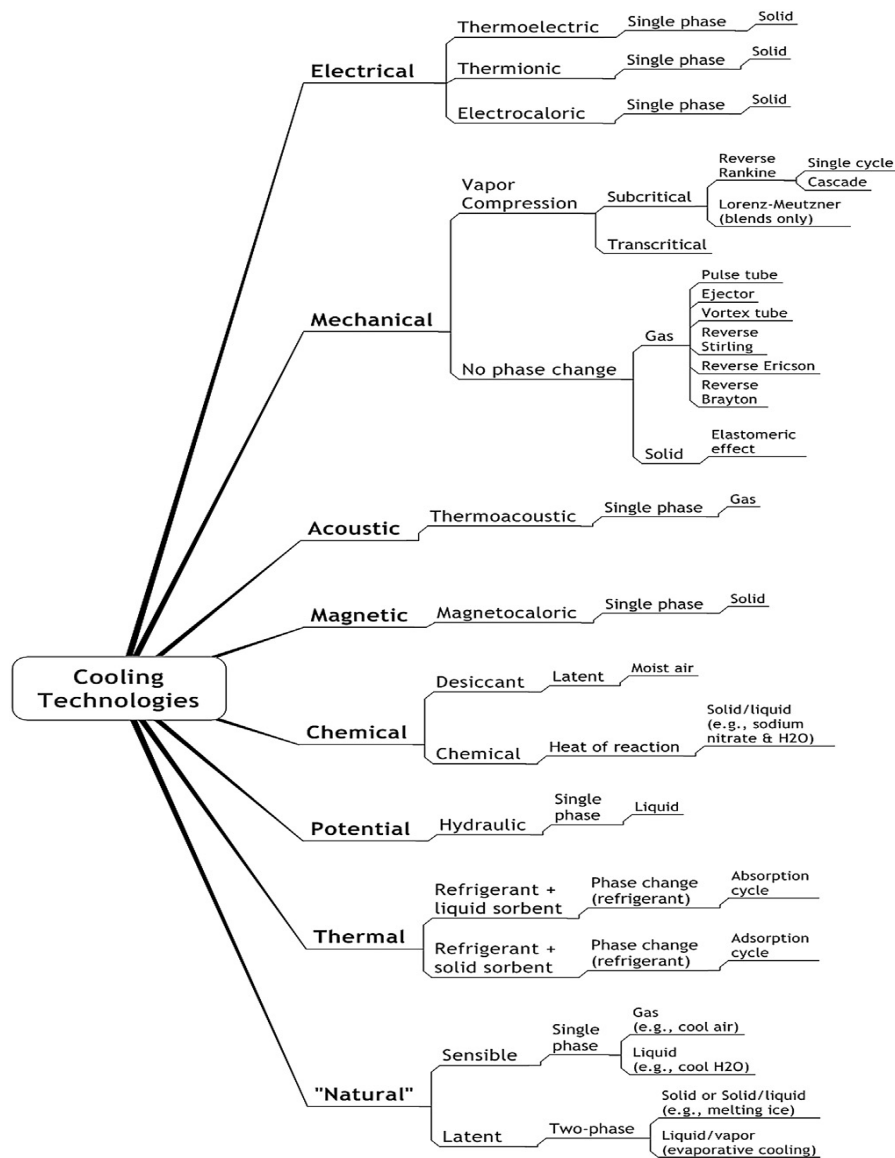


Figure 1. Cooling Technologies Classification(Steven Brown & Domanski 2014)

Vortex tube cooling systems (VTCS) is a mechanically driven alternative cooling system that can be used to create both heating and cooling effects, without causing any harm to the environment.(Steven Brown & Domanski 2014) Using compressed air as the working fluid is the primary advantage of a vortex tube refrigeration system. The vortex tube has been referred to by a variety of different names over the years. Names such as Ranque vortex tube, Hilsch vortex tube, Ranque–Hilsch tube and Maxwell–Demon tube (derived from the name of Maxwell and Demon group who together studied the molecule of hot air moving within the tube). The Ranque-Hilsch effect governs the operation of the Vortex tube.(Xue 2012) This effect describes the temperature distribution in a confined, constantly rotating fluid flow. The vortex tube refrigerator comes with pre-calibrated gauges and valves. With the intake nozzle with a four-way tangential inlet spaced at 90 degrees, the vortex tube's hot and cold ends are connected by an orifice and a control valve. The first step is to open the nozzles so that high-pressure air may flow through. When a fluid goes through the nozzles, its velocity increases (it is estimated to be more than 1 million rpm).

This high velocity causes the tube to follow a circular route around its circumference. A little amount of fluid is redirected to flow in the tube's middle after passing through the heated end, where it slows down and begins to flow counterclockwise. A pressurized gas is injected into a vortex tube, which then produces cold and hot streams. Interesting phenomena like energy separation occur only because of fluid dynamics in the tube, not mechanical

movement, or chemical reaction. Some research and experimental works have made attempt on the explanation of the low temperature variation and energy separation phenomenon of vortex tube cooling system, while others have looked at the design, fabrication, and performance analysis under geometrical and thermophysical characteristics of the vortex tube. But this research will try to combine these approaches into a single study with the aim to achieve the objective stated in section 1.1.

1.1 Objectives

This study concentrates on a vortex tube cooling system (VTCS) design, fabrication, performance test and validation of the experimental result via simulation. It envisages the possibility of identifying some directions for future research, while it provides discussion to support existing works that have been done in this regard.

2. Literature Review

An overview of geometrical, thermophysical, and prior investigations into temperature separation in the vortex tube, including experiments and simulations, is also included in this section. The physical behavior of the flow remains a mystery due to its complexity and conflicting experimental results, despite many experimental and numerical research on vortex tubes.

2.1 Review Studies

Presented below in table 1.0 are summary of previous studies on either review or experimental and numerical studies of the vortex tube. This literature will serve as the basis to undertake this study.

Table 1. Selected Studies on Vortex Tubes

Reference	Findings and Summary
(Nangare et al. 2021)	This research examines and proposes a wide range of applications for the vortex device, which is of interest to researchers around the world. There has been some interest in producing hot or cold gases without the use of a mechanical mechanism in the literature, though. An extensive range of uses for vortex tubes has been documented in this research. According to this collection of studies, counter-flow vortex tubes can be used to recover energy from compressed gas and to meet specific application needs in a certain industry.
(Chýlek et al. 2018)	This study compares computational and experimental simulations of vortex tubes. Star-CCM+ was utilized for the CFD simulations. The numerical analysis made use of models based on three-dimensional geometry and turbulence physics. A vortex tube experimental device was created and tested in order to verify computations. There was a comparison between simulation and experiment results for Standard k, Realizable k-, SST k-, and the Reynolds stress model (RSM). The most crucial assessor was the temperature of the vortex tube. The flow through the vortex tube was exactly predicted by all turbulence models. The best temperature distribution was predicted by the standard k-turbulence model.
(Karthikeya Sharma et al., 2017)	This paper presents computational analyses of vortex by many researchers, along with results and suggestions to improve vortex tube performance. This paper discussed turbulence models that accurately predict performance. LES, k- ϵ , k- ω , and RMS were used to predict vortex tube energy separation. Some researchers used ANN and Taguchi for analysis. Comparisons of predictions with simulation results were also presented to show the CFD models' prediction abilities.
(Nikitin et al. 2015)	The review provides a concise summary of the computational fluid dynamics (CFD) methods utilized for Ranque–Hilsch vortex tube numerical analysis. Fluid dynamics in the vortex tube are difficult to model numerically because of the complicated whirling fluid flow. More computing power and more precise CFD setups can improve the correlation between experimental and simulated data. Gas flow analysis is hampered by a lack of credible theoretical background on the Ranque–Hilsch vortex phenomenon.
(Dutta et al. 2011)	A three-dimensional CFD model is used to explore how energy and species segregate in a vortex tube (VT) using ambient and cryogenic air. This study uses a real gas

	model to get precise thermodynamic and transport characteristics in the VT. CFD uses perfect gas law. Hot and cold outlet temperatures vs hot outlet mass fraction are compared to ambient data. Separating oxygen and nitrogen from air is ineffective. At cryogenic temperatures, energy and species are closer.
(Eiamsa-ard & Promvong 2008)	The vortex tube's geometrical, thermo-physical, and temperature separation were reviewed using experiments and simulations. Quantitative, theoretical and analytical components of the topic are examined in the computing review. Vortex tube flow behavior remains a mystery despite numerous experimental and numerical investigations due to its complexity and the inconsistent nature of experimental results. For the thermal separation phenomena, various distinct ideas have been put forward based on experimental, analytical and numerical studies.
(Chang-Hyun et al. 2006)	In this study, experimental testing and numerical modeling are used to examine the internal flow of a counterflow vortex tube. Dye was injected into the vortex tube for visualization. Vortex tubes are made of acrylic, and air pressure can be varied from 0.1MPa to 0.3MPa to trace surface particles. Every experimental test showed a sudden change in a vortex tube's path. This could mean the vortex has stopped moving. Increasing cold flow rate and input pressure move stagnation closer to the vortex generator. In order to get more accurate flow data, the vortex tube is also analyzed in 3D. Experimental values of pressure, temperature, and pressure distributions in the vortex tube matched the numerical computation well. The computational particle trail matches the experimental one.

3. Materials and Methods

Materials

The scope of this work is limited to the design and production of a simple vortex tube cooling system (Counter-flow type) using locally available raw material, Unplasticized Polyvinyl Chloride (uPVC) pipes. This uPVC material for the vortex tube was chosen because of the important properties which it possesses that includes low thermal conductivity, low weight, excellent corrosion resistance and easily machinable. Other components of the VTCS as selected in the design, with reasons for their choices are presented in table 1.1 below.

Table 1.1 Component and Working Parts of the Vortex Tube

S/No	Parts	Materials Used	Reason for Choice	Working
1.	Hot tube end	uPVC	<ul style="list-style-type: none"> • Thermal conductivity. • Thermal insulation. 	<ul style="list-style-type: none"> • This serves as a conveyor for carrying the swirling compressed air. Energy separation also takes place within the hot tube.
2.	Vortex Chamber	uPVC	<ul style="list-style-type: none"> • For uniformity and weldability. • Homogeneity and easy joining with other parts. 	<ul style="list-style-type: none"> • This part houses the spinner. Air goes through it to the hot tube.
3.	Spinner	Perspex	<ul style="list-style-type: none"> • Easy to cut by available CNC machining to precision 	<ul style="list-style-type: none"> • The spinner is the part that induces swirling motion to the impinging compressed inlet air.
4.	Conical Valve	Perspex	<ul style="list-style-type: none"> • Easy to cut by available CNC 	<ul style="list-style-type: none"> • This is important in the counter flow vortex tube in causing

			machining to precision	the exit for the hot air and a rebounding surface for the cold air in the inner vortex. It is often used to control the amount of cold air mass ratio; this is done by making it moveable in the longitudinal axis of the hot tube. As seen in the working drawing in the appendix, the cone valve is made in steps. This choice is to give a surface normal to the cold air vortex to ensure maximum cold air rebound.
5.	Cold tube end	uPVC	<ul style="list-style-type: none"> • Thermal conductivity. • Low thermal conducting property. 	<ul style="list-style-type: none"> • This is a tube that conveys the cold air after it has passed the orifice.
6.	Air inlet	Steel with half coated rubber		
7.	Digital temperature sensor			
8.	Air compressor (with pressure regulator and pressure regulator)			
9.	Supporting frame	Wood	<ul style="list-style-type: none"> • Cost effectiveness • Adequate strength • Low weight. 	<ul style="list-style-type: none"> • The supporting frame bears the vortex tube and the experiment accessories.
10	Cold air orifice			<ul style="list-style-type: none"> • this is a hole that allows the cold air to leave the hot tube after bouncing off the cold valve.
11	Nozzle			<ul style="list-style-type: none"> • This part allows the air from the compressor to be introduced into the vortex chamber with minimal pressure loss.

Empirical Models and Important Definitions Used with Vortex Tube Design

In this study, an attempt will be made to construct the Ranque-Hilsch Vortex Tube model using uPVC. Many of the most often used words in Vortex tube cooling system design and performance evaluation research and in this study are outlined here.

- Cold mass fraction (ζ): represents the mass of air discharged at the cold end of the tube to the total compressed air supplied to the tube, and given by:

$$\zeta = \frac{\text{mass flow of air at the cold end}}{\text{total mass flow of air supplied to vortex tube}}$$

- Cold and hot temperature difference: a variation in temperature between the intake and outlet flows

$$\Delta T = T_{in} - T_c$$

Where T_{in} and T_c are the inlet flow temperature and cold flow temperatures, respectively

- Isentropic efficiency: the process inside the RHVT is assumed to be isentropic expansion, and the Isentropic efficiency is given as.

$$\eta_{is} = \frac{h_{in} - h_c}{h_{in} - h_s}$$

- Coefficient of Performance (COP): the coefficient of Performance (COP) as a refrigerator is defined as the ratio of the cooling power gained by the system to the work power is given by;

$$COP_{cr} = \frac{\dot{Q}_c}{\dot{W}}$$

Here the cooling power can be calculated according to the cooling capacity of the cold exhaust gas (e.g. the heat necessary to heat up the cold exhaust gas from the cold exhaust temperature to the applied temperature)

$$\dot{Q}_c = \dot{m}_c c_p (T_{in} - T_c)$$

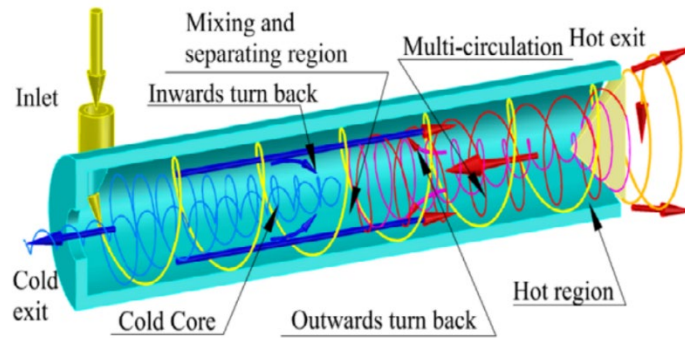


Figure 1.2. Counter Flow Vortex Tube Showing Important Components (Yunpeng et al. 2015)

Design Parameters

In the design, the parameter used are presented in the table 1.2 below.

Table 1.2. Design parameters adopted for the present study

Design Parameters	Values
Nozzle area to tube diameter ratio	0.11
Cold orifice area to tube area	0.080
Length to diameter ratio of tube	45 - 55
Length to diameter ratio (L/D)	9.3 (L=106mm)
Cold mass fraction (ζ)	0.288
No of nozzles	3
Diameter of nozzles	D/3
No of nozzles	2
Diameter (D)	12.70mm (0.5 inch)
Length of cold tube	10D
Length of hot tube	45D
Cold orifice diameter	0.5D

Design Problems Encountered in the VTCS Design

- **Turbulence:** High speed rotating flows generally have high level of turbulence. Due to this turbulence the energy transfer rate reduces considerably.
- **Vortex breakdown:** Under certain conditions, rotating flows in ducts are seen to undergo a dramatic change as they progress along the duct. Such a change is known as a vortex breakdown and generally takes one or two forms. At moderate swirl Reynolds numbers and with low turbulence a stable axisymmetric ‘bubble’ breaks down was found. This makes haphazard flow inside the tube causing a less amount of energy separation within the vortices.
- **Inertial waves:** Fluids whether incompressible or otherwise, rotating geotropically with an angular velocity (ω) can support inertial waves with angular frequencies up to (2ω) . In a rotating flow moving axially through duct inertial waves provide a mechanism for the upstream transmission of information where their phase velocity exceeds the axial velocity of the fluid.
- **The Vortex Whistle:** A tone being produced by swirling flows passing from containing ducts into the still atmosphere. The sound was termed as Vortex Whistle. This sound accelerates vortex breakdown inside the tube which cause further reduction in the temperature drop

3.1 Fabrication and Assembly of the VCTS

Hot Tube and Vortex Chamber

Using a tube of 10.5mm internal diameter, thickness of 1.25mm, and a length of 625mm as required for the hot tube end of the vortex tube, thereafter it was marked and cut using a scribe and cutting machine and the right fitting were selected to serve as the sockets, accordingly. The extended ends of the tube having the sockets served as the side plate for the vortex chamber and was therefore drilled to allow space for nozzle installation.

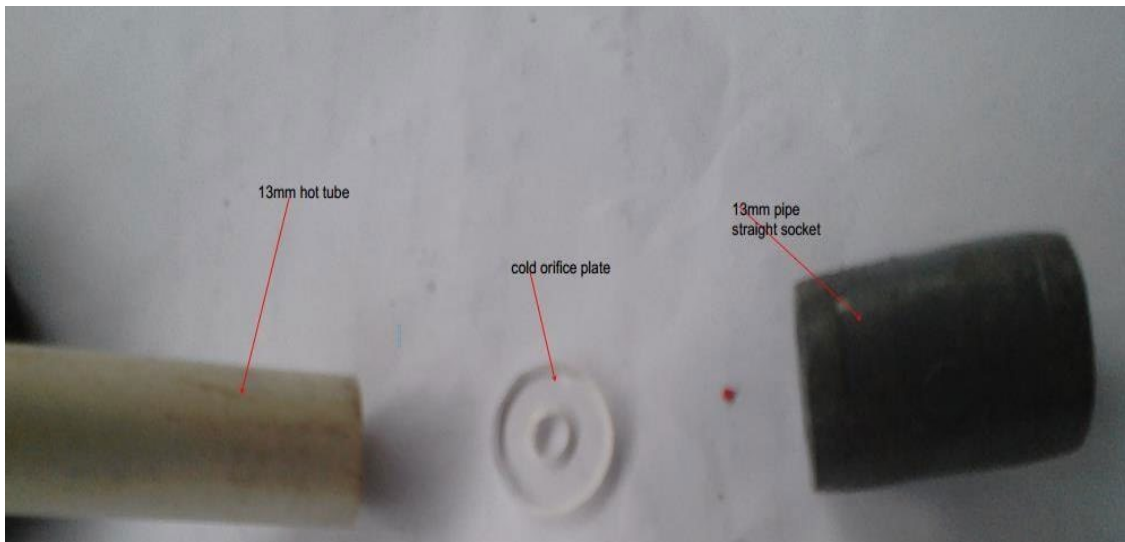


Figure 1.3. The Hot Tube, Socket and Orifice Plate are fabricated to form the Vortex Generator by drilling through tangentially

Spinner

By the advantage of the thickness of the PVC material, the spinner was not made as an external component. Fixing the hot tube into a 13mm socket, holes tangential to the internal surface of the hot tube were drilled through the surrounding socket. This was sufficient in inducing swirl in the incoming compressed air, though the flow profile is expected to be different from that in the other material models.

$$\text{Tangential hole diameter} = 13 \times 0.11 = 1.43\text{mm (taken as 1.5mm, available drill bit size)}$$

Cold Orifice

This had to be a separate component. Here, a flat Perspex plate was marked a circle of diameter 13mm, the diameter of the hot tube, with its circumferential thickness. It was cut and smoothed using a file. A hole of 6.5mm was drilled at the center of the prepared plate.

$$\text{Hole diameter} = 0.5 \times 13\text{mm.}$$

Cold Tube

Another 30mm length of the 13mm PVC pipe was cut to serve as the cold tube end.

Cone Valve

This part was produced using the CNC Lathe. The work piece (Perspex rod of diameter 20mm) produced is in steps with each of the steps varying in diameters and its successive distances.

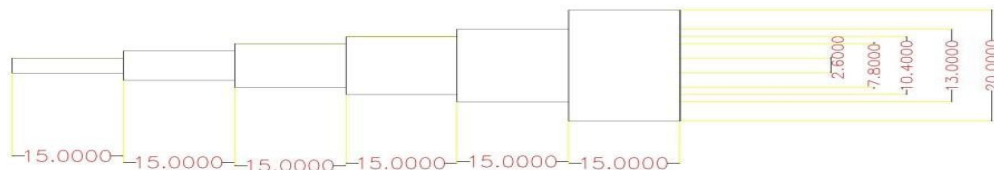


Figure 1.4. Diagram of Cone Valve

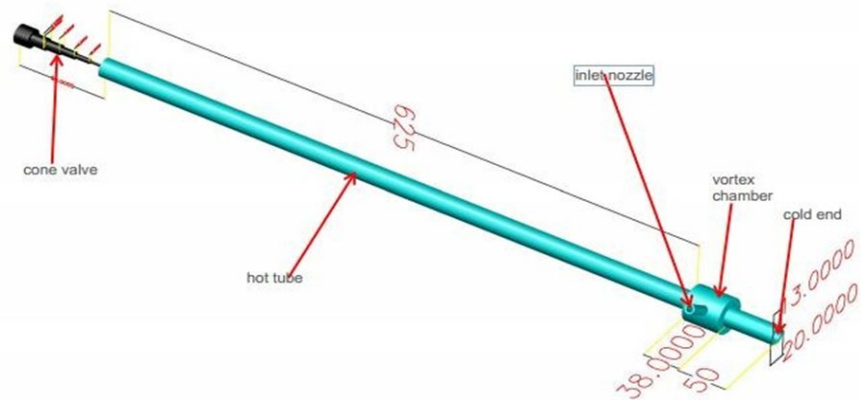


Figure 1.5. Assembly of the uPVC Vortex Tube Model Showing Important Components

3.2 Experimental Set-Up

The set-up of the apparatus used for the experiment is shown in figure 1.6 below.



Figure 1.6. Set-up of the VCTS Experiment

a = air compressor, b = pressure regulator, c = pressure gauge, d = hose, e = vortex tube, f = hot end, g = hot end valve, h = cone valve stand, i = cold end, j = temperature sensors.

4. Experimentation and Procedures

The experiments were done to demonstrate the behavior of the vortex tube based on the temperature at the hot ends and cold ends when the pressure of the ambient air is varied and when the hot air mass fraction by cone valve length are varied separately.

4.1 Experiment 1: Effect of Hot Air Mass Fraction on the Vortex Tube Cooling

4.1.1 Objective: To investigate the effect of air mass fraction on temperature separation for the uPVC vortex tube.

4.1.2 Apparatus: uPVC vortex tube set, 2.5Hp compressor with pressure gauge and pressure regulator, digital thermometers, stopwatch.

4.1.3 Procedures:

- a. The ambient air temperature reading was taken and recorded.
- b. The air compressor was connected to the power supply mains and the power knob on it, pulled up to set it to work.
- c. The compressor supply pressure was set to 3bar.
- d. The temperature reading at the air inlet hose of the compressor was taken and recorded.
- e. The digital temperature sensor probes were brought close to the ends of the hot and cold tubes respectively and fastened using a piece of masking tape.
- f. The air compressor and the digital temperature sensors were SWITCHED ON.
- g. The cone valve was varied from each step-turning diameter of the valve 20%, 40%, 60%, and 80% of the hot-end opening.
- h. For these respective percentage openings, their temperatures were recorded as displayed on the Digital Temperature Sensor.

4.2 Experiment 2: Effect of Pressure of Supplied Air on Energy Separation and Cooling in the Vortex Tube

4.2.1 Objective: To investigate the effect of the pressure variation on the ambient air on the temperature separation of the vortex tube.

4.2.2 Apparatus: uPVC model vortex tube set, 2.5hp compressor with pressure gauge and pressure regulator, digital temperature sensors, masking tape, stopwatch.

4.2.3 Procedures:

- a. The air compressor with a power rating of 2.5 hp was attached to the air inlet nozzle through its hose.
- b. The digital temperature sensor probes were brought close to the ends of the hot and cold tubes respectively and fastened using the masking tape.
- c. The air compressor was turned on while its exit was kept closed to allow air to fill its storage cylinder.
- d. The digital temperature sensors were SWITCHED ON.
- e. The air compressor outlet pressure is set to 1bar using the pressure regulation valve and monitoring with the pressure gauge.
- f. The values for the temperature of both ends of the vortex tube were recorded as displayed on the digital thermometer displays, T_h for the hot end, and T_c for the cold end readings respectively.
- g. The compressor supply pressure, P , was changed between 1 to 6 bar, and respective temperature reading for the hot end and cold end were recorded accordingly.
- h. The cone valve position was adjusted to 20%, 40%, 60%, and 80% hot air shut out and steps (f) and (g) were repeated respectively for the adjusted cone valve position.

4.3 Numerical Simulation with ABAQUS

The conservation of mass, momentum, and energy define compressible turbulent flows in the vortex tube. The vortex tube's flow is extremely turbulent. The following is the solution to the conservation of mass and momentum, as well as the equation's current state:

$$\frac{\partial}{\partial t}(\rho) + \frac{\partial}{\partial x_j}(\rho \tilde{u}_j) = 0$$

$$\frac{\partial}{\partial t}(\rho u_i) + \frac{\partial}{\partial x_j}(\rho \tilde{u}_j u_i - \tau_{ij}) = -\frac{\partial p}{\partial x_i}$$

$$p = \rho RT$$

Simulation of the flow properties of the inlet air as well as the flow in the hot tube was examined using ABAQUS software. The velocity, vorticity, and pressure distribution of flow were simulated and analyzed. A simulation was also done for pressure distribution, temperature separation in the simulated air boundary whose geometry is the same as the physical prototype built. This enabled the comparison between the values of the physical model and the finite element analysis model. From this comparison, a deduction on the input parameters for optimal performance on the built vortex tube was made.

Procedures:

- Compressed air passing through the Vortex Tube was modeled.
- The model of the compressed air was reduced into small and unique parts known as finite elements.
- Variables of interest were then calculated (Temperature, Pressure, and Velocity) at the nodes of the elements.
- The results of the variables were then displayed using different colors.
- Modeled air space boundary was the internal volume of the designed vortex tube from the air inlet nozzle limited at the hot and cold ends.

4.4 Precautions Observed in the Experiments

- Some precautions observed when the experiment was carried out included:
- The air compressor was intermittently stopped so that it does not get too heated up, which was observed to cause instability in the temperature separation.
- There was no attempt to exceed the pressure specification of the compressor-8 bar.
- Two thermometers were used simultaneously to read the temperature of the cold end and the hot end.
- Sufficient time was allowed for the thermometer reading to stabilize before the measurement was taken.
- With the absence of a flowmeter, adjustment at the compressor exit valve was made for flow rates, and the average was taken.
- Air leakages were thoroughly guarded against.
- The condensed water in the tank of the air compressor was removed at the end of the experiment.
- The probe of the thermometer was not touched with the hands to avoid disturbances.

5. Results, Validation and Discussion

The results of the experiments 1 and 2 are therefore presented in section 5.1.1 and 5.1.2 in tables 1.5 to 1.9.

5.1.1 Experiment 1

Table 1.3. Temperature separation while varying hot air mass fraction at constant pressures (1 bar) and constant temperatures profiles at hot end and inlet-air.

S/N	Pressure (bar)	Blockage of the hot end (%)	Inlet Compressed Air Temperature, T_s (°C)	Cold-End Temperature, T_c (°C)	Hot-End Temperature, T_h (°C)	Cooling Effect, $(T_s - T_c)$ (°C)
1	1	20	32.0	29	30.7	3.0
2	1	40	32.0	28.7	29.8	3.3
3	1	60	32.0	28.5	29.3	3.5
4	1	80	31.7	24.7	28.1	7.0

Table 1.4. Temperature separation while varying hot air mass fraction at constant pressures (2 bar) and

constant temperatures profiles at hot end and inlet-air

S/N	Pressure (bar)	Blockage of the hot end (%)	Inlet Compressed Air Temperature, T_s (°C)	Cold-End Temperature, T_c (°C)	Hot-End Temperature, T_h (°C)	Cooling Effect, ($T_s - T_c$) (°C)
1	2	20	32.0	28.9	30.7	3.1
2	2	40	32.0	28.7	29.8	3.3
3	2	60	32.0	28.4	29.3	3.6
4	2	80	31.7	22.8	28.1	8.9

Table 1.5. Temperature separation while varying hot air mass fraction at constant pressures (3 bar) and constant temperatures profiles at hot end and inlet-air

S/N	Pressure (bar)	Blockage of the hot end (%)	Inlet Compressed Air Temperature, T_s (°C)	Cold-End Temperature, T_c (°C)	Hot-End Temperature, T_h (°C)	Cooling Effect, ($T_s - T_c$) (°C)
1	3	20	32.0	28.6	30.7	3.4
2	3	40	32.0	28.4	29.8	3.6
3	3	60	32.0	28.3	29.3	3.7
4	3	80	31.7	22.3	28.1	9.4

Table 1.6. Temperature separation while varying hot air mass fraction at constant pressure (4 bar) and constant temperatures profiles at hot end and inlet-air

S/N	Pressure (bar)	Blockage of the hot end (%)	Inlet Compressed Air Temperature, T_s (°C)	Cold-End Temperature, T_c (°C)	Hot-End Temperature, T_h (°C)	Cooling Effect, ($T_s - T_c$) (°C)
1	4	20	32.0	28.5	30.7	3.5
2	4	40	32.0	28.1	29.8	3.9
3	4	60	32.0	27.8	29.3	4.2
4	4	80	31.7	22.3	28.1	9.4

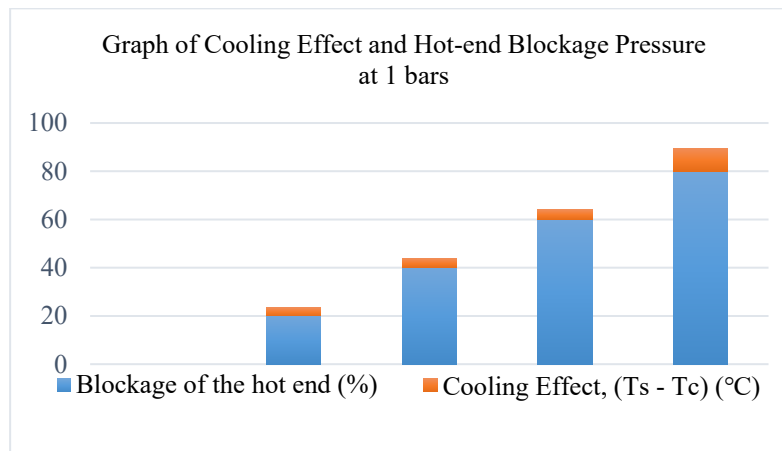
5.1.2 Experiment 2

Table 1.7 Temperature separation at constant hot tube end while varying pressure at constant hot-end blockage of 80%

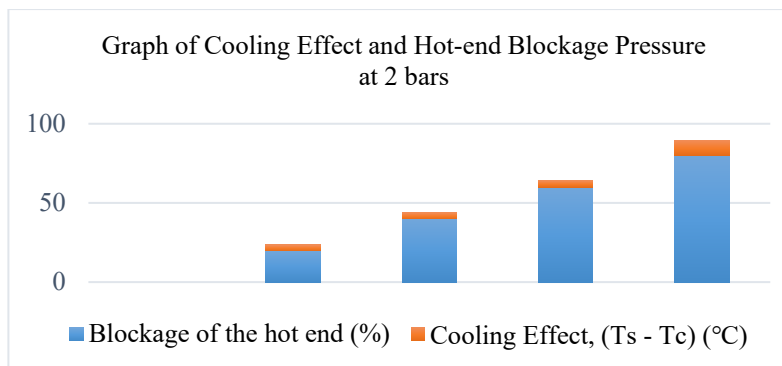
S/N	Pressure (bar)	Blockage of the hot end (%)	Inlet Compressed Air Temperature, T_s (°C)	Cold-End Temperature, T_c (°C)	Hot-End Temperature, T_h (°C)	Cooling Effect, ($T_s - T_c$) (°C)
1	1.0	80	29.2	27.1	28.4	2.1
2	2.0	80	32.3	28.2	30.0	4.1
3	3.0	80	33.0	29.3	30.2	3.7
4	4.0	80	34.3	29.3	31.1	5.0
5	5.0	80	33.4	30.9	31.6	2.5
6	6.0	80	28.5	26.2	28.3	2.3

5.2 Graphical Results

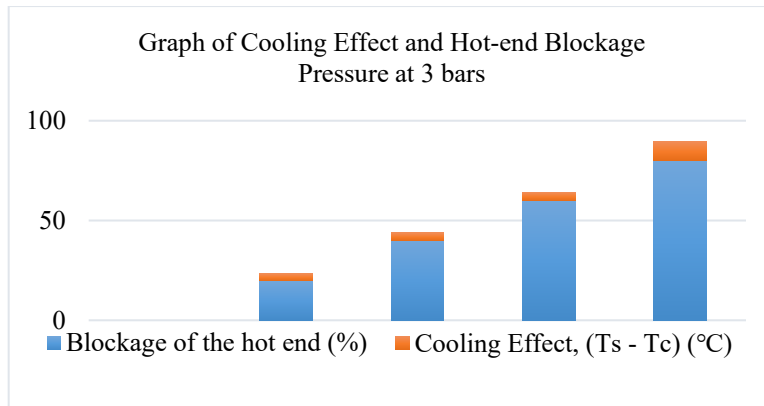
The results obtained in the experiments are represented by the following graphs in figure 1.7 below.



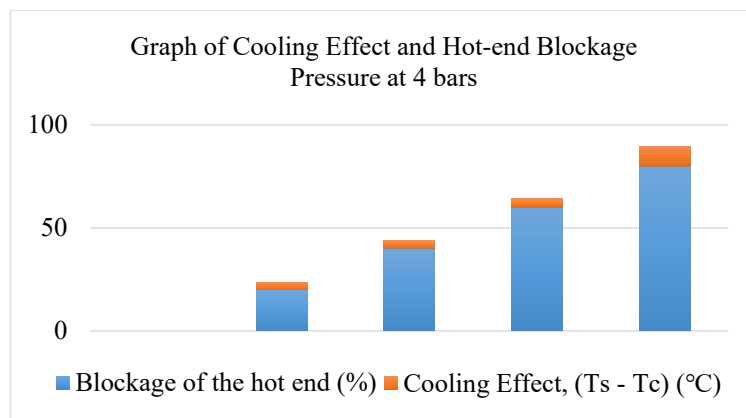
(a) Pressure at 1 bar



(b). Pressure at 2 bar



(c). Pressure at 3 bar



(d). Pressure at 4 bar

Figure 1.7 (a)-(d). Graph of cooling effect against blockage of hot end of the vortex tube

Figure 1.7 shows that maximum cooling was achieved at 80% blockage of the hot end after varying the pressures from 1 to 4 bar.

Consequently, and with these results, different pressures values (from 1 to 6 bars) were applied at the 80% hot end blockage, to determine which pressure will produce the best maximum cooling. The result as obtained in table 1.9 is therefore represented in figure 1.8 below.

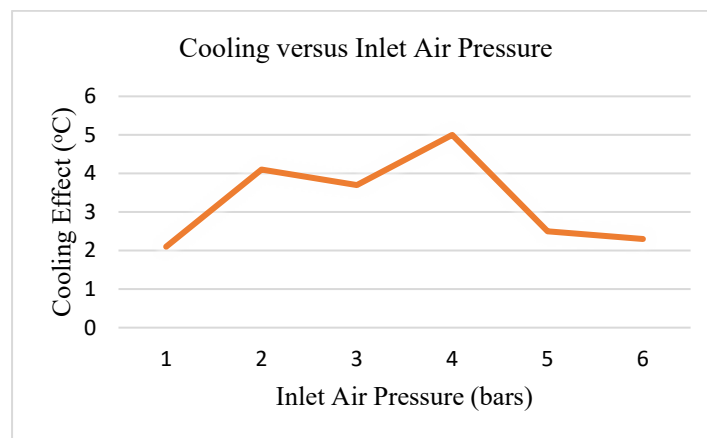


Figure 1.8: Graph of cooling achieved against inlet air pressure at 80% hot tube end blockage

5.3 Numerical Simulation Findings

5.3.1 Input Variables as used in the Simulation:

Based on the experimental parameters used in achieving maximum cooling, the values were used for the modelling and numerical simulation.

Table 1.8. Variables as used in the Simulation

Variables	Units
Hot-end Temperature	31.7°C
Mass flow rate	504.3 m ³ s ⁻¹

The results of the simulation procedures as followed in section 4.3.1 are presented below in figure 1.9 and 2.0.

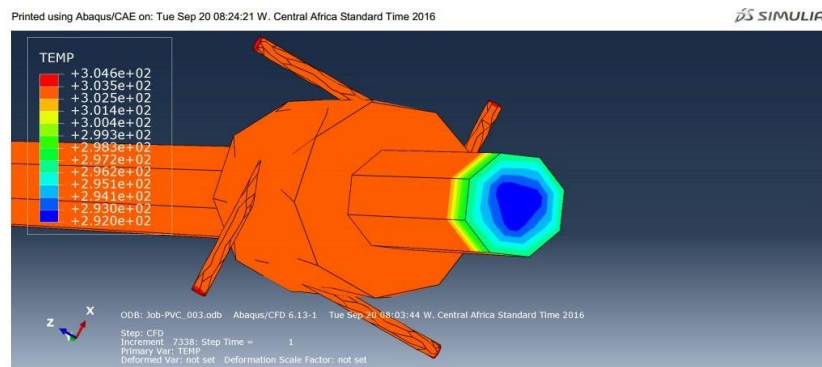


Figure 1.9. ABAQUS model simulation result for temperature distribution at the cold end using 80% hot end blockage and mass flow of 504.3 m³/s

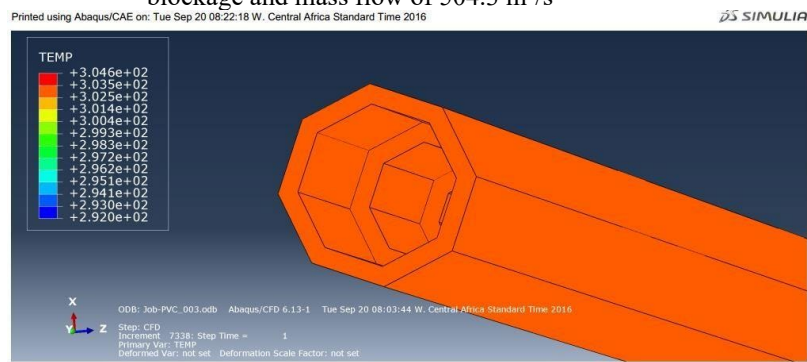


Figure 2.0. ABAQUS model simulation result for temperature distribution at the hot end of the vortex tube at maximum cooling

5.4 Discussion

5.4.1 Vortex Tube Behavior

From the data in Experiment 1, 80% blockage of the hot end gave the highest cooling effect of 9.4 which was a cold end temperature of 22.3°C, at an inlet temperature of 31.7°C. The value of hot air mass blockage (80%) was used in Experiment 2 as a constant, while the pressure was varied. From the graph, 4 bars gave the highest cooling effect. This 80% blockage also gave the highest cooling in the ABAQUS simulation but with a value of $2.92 \times 10^2 \text{ K} = 292 \text{ K} = 19^\circ \text{C}$ at cold end and different pressure values. Hence, it was inferred as the percentage blockage for hot air mass to achieve maximum cooling is valid. This value of pressure with the highest cooling effect in the experiment compared to the simulated value had a difference of 1.08 bar. The ABAQUS computed inlet pressure at maximum cooling was 2.92 bar compared with 4 bars obtained from the experiments. There was a non-linear relation between the input pressures to the cooling effect achieved. Up to 4bar, there was a steady increase in cooling with pressure, beyond 4 bar

a negative relation was noticed in the simulation. This explains the behavior of the vortex cooling tube phenomenon described by (Eiamsa-ard & Promvonge, 2008) (Karthikeya Sharma et al., 2017), as possessing uncertainties.

5.4.2 Flow Profile

From the ABAQUS simulated profile, the swirl was seen throughout the length of hot tube confirming the validity of the proposed swirling profile of the injected air in the vortex tube. The correctness of our design was also proven by this. The cold air was seen as also having swirls as anticipated. The velocity of inlet air at the maximum cooling was 590m/s.

5.5 Proposed Improvements

Since numerical modelling suffers from some limitations, including the disparity between simulation results and those obtained in this research experiments. A traditional k- turbulence model that was somewhat modified by (Bazgir et al., 2019) revealed that the vortex tube had a clear energy separation effect, and the numerical solutions of the flow and temperature fields matched well with the experimental results.(Liu et al., 2005). Therefore, an integration of Design of Experiment approach to generate multiple structured data set for the variable of the vortex tube to studying, evaluating, and doing a sensitivity analysis on the pattern and effects of both experimental and numerical simulation test results for the Vortex Cooling Tube.

6. Conclusion and Future Work

Here in this research, an attempt is to be made on building the Ranque-Hilsch Vortex Tube model using uPVC material. Analysis on the temperature separation as a function of the hot air mass fraction and the inlet air pressure were tested and the results proved satisfactory and showed agreement with similar works done previously by researchers. High noise and low thermal efficiency are the main limitations of industrial use of the vortex tube.(Eiamsa-ard & Promvonge, 2008)(Kurosaka M, 1982). The author in (Kurosaka M, 1982) found an acoustic streaming phenomenon involving a vortex tube, which produced noise levels of up to 125 dB from the vortex tube's noise source. Vortex tubes may be doomed if these issues continue to be present. A study found that the vortex tube's thermal efficiency peaked at 30%, which is significantly lower than that of other thermal devices. Since the vortex tube is less efficient, its industrial uses are more limited. The vortex tube is suitable for application where compactness, low cost and small areas of cooling are involved. The effect of material properties on the performance of the vortex tube could be examined and a comparison made with this work. The maximum mass flow rate of the air compressor of 120l/min (432 cubic meter per second) was maintained throughout this research. Examination of the effect of the mass flow rate on the temperature separation is highly recommended. Also, cascading the vortex tube like cascading compressor blade sets to obtain better performance could also be explored. While the study of vortex tube flow phenomenon is still a bit difficult to fully have a unified result with little or no discrepancies, despite multiple experiments and computer simulations, a research direction in undertaking a sensitivity analysis of results from vortex tube repeated experimental and simulation results can possibly provide a clear insight into the underlying reasons for the inconsistencies.

References

- Bazgir, A., Khosravi-Nikou, M., & Heydari, A., Numerical CFD analysis and experimental investigation of the geometric performance parameter influences on the counter-flow Ranque-Hilsch vortex tube (C-RHVT) by using optimized turbulence model. *Heat and Mass Transfer/Waerme- Und Stoffuebertragung*, 2019. <https://doi.org/10.1007/s00231-019-02578-1>
- Brown, J. S., & Domanski, P. A., *Alternative Cooling Technology Options* (pp. 1–8). National Institute of Standards and Technology, 2011.
- Chang-Hyun, S., Chang-Soo, K., Ui-Hyun, J., & B.H.L Lakshmana, G., Experimental and Numerical Studies in a Vortex Tube. *Journal of Mechanical Science and Technology (KSME Int. J)*, 20(3), 418–425, 2006.
- Chýlek, R., Šnajdárek, L., & Pospíšil, J., Vortex Tube: A Comparison of Experimental and CFD Analysis Featuring Different RANS Models. *MATEC Web of Conferences*, 168, 2018. <https://doi.org/10.1051/mateconf/201816802012>
- Dutta, T., Sinhamahapatra, K. P., & Bandyopadhyay, S. S., Numerical investigation of gas species and energy separation in the Ranque-Hilsch vortex tube using real gas model. *International Journal of Refrigeration*, 34(8), 2118–2128, 2011. <https://doi.org/10.1016/j.ijrefrig.2011.06.004>
- Eiamsa-ard, S., & Promvonge, P., Review of Ranque-Hilsch effects in vortex tubes. In *Renewable and Sustainable Energy Reviews* (Vol. 12, Issue 7, pp. 1822–1842), 2008. <https://doi.org/10.1016/j.rser.2007.03.006>

- Karthikeya Sharma, T., Amba Prasad Rao, G., & Madhu Murthy, K., Numerical Analysis of a Vortex Tube: A Review. *Archives of Computational Methods in Engineering*, 24(2), 251–280, 2017. <https://doi.org/10.1007/s11831-016-9166-3>
- Kurosaka M. (1982). Acoustic streaming in swirling flow and the Ranque-Hilsch (vortex-tube) effect. In *J. Fluid Mech.*
- Liu, J. Y., Gong, M. Q., Zhang, Y., Hong, H., & Wu, J. F. (2005). Numerical Research on a Special Fluid Phenomenon: Ranque-Hilsch Effect. *Modern Physics Letters B*, 19, 1723–1726. www.worldscientific.com
- Nangare, S. S., Pharande, V., & Ghadage, S. S. (2021). *Review on Applications of Vortex Tube Refrigerator* (Vol. 8). JETIR. www.jetir.org
- Nikitin, V., Bogdevičius, P., & Bogdevičius, M., Overview of Numerical Methods for Simulating Ranque-Hilsch Effect within Vortex Tubes. *Mokslas – Lietuvos Ateitis*, 7(5), 571–576, 2015. <https://doi.org/10.3846/mla.2015.830>
- Steven Brown, J., & Domanski, P. A., Review of alternative cooling technologies. *Applied Thermal Engineering*, 64(1–2), 252–262, 2014. <https://doi.org/10.1016/j.applthermaleng.2013.12.014>
- Xue, Y. (2012). *The working principle of a Ranque-Hilsch Vortex Tube* [University of Adelaide]. <https://digital.library.adelaide.edu.au/dspace/bitstream/2440/82139/8/02whole.pdf>
- Yunpeng, X., Mehdi, J., Amanullah, C., & Maziar, A. (2015). The Expansion Process in a Counter-flow Vortex Tube. *Fluid Mechanics: Open Access*, 02(01), 2015. <https://doi.org/10.4172/2090-8369.1000114>

Biographies

Joseph Akpan is currently a Master's student in the Department of Industrial Engineering, Durban University of Technology (DUT), South Africa with a Bachelor's in Mechanical Engineering from the University of Uyo, Nigeria. Prior to his present studies, he worked shortly as a Graduate Engineering Intern at ExxonMobil Nigeria, where he had grown to develop interests in committing to research findings, exploring industry 4.0 technologies towards physical asset management, energy systems optimization, and engineering education. He is a Certified Maintenance & Reliability Professionals (CMRP), graduate student member of the Society of Maintenance & Reliability Professionals (SMRP), American Society of Engineering Management (ASEM), and the Nigerian Society of Engineers (NSE).

Edwin Umo is an engineering graduate intern at Notore Chemical Industries, Nigeria and is building competence in equipment process operation and maintenance for gas and urea granules production. He is also a recent graduate of Mechanical Engineering from the University of Uyo, Nigeria. He has interest in materials science and computational aided engineering, green energy systems design and implementation. He is a graduate member of the Nigerian Society of Engineers (NSE).

Oludolapo Akanni Olanrewaju is currently a Senior Lecturer and Head of Department of Industrial Engineering, Durban University of Technology, South Africa. He earned his BSc in Electrical Electronics Engineering and MSc in Industrial Engineering from the University of Ibadan, Nigeria and his Doctorate in Industrial Engineering from the Tshwane University of Technology, South Africa. He has published journal and conference papers. His research interests are not limited to energy/greenhouse gas analysis/management, life cycle assessment, application of artificial intelligence techniques and 3D Modelling. He is an associate member of the Southern African Institute of Industrial Engineering (SAIIE) and NRF rated researcher in South Africa.

Victor Okorie is a field service engineer with P.E.T Associates Limited where he provides technical and engineering support for HVAC systems operations across clients' sites. He is also a recent graduate of Mechanical Engineering from the University of Uyo, Nigeria. His interest spans across design, operations and maintenance of heating & cooling systems, sales and project engineering. He is a graduate member of the Nigerian Society of Engineers (NSE).